Journal of Energy & Environment 3 (2004) 15 - 24

Heat Transfer Analysis and Pressure Drop Correlations for the Double-Pass Solar Collector with Porous Media

Elradi A. Musa, K. Sopian and Shahrir Abdullah
Mechanical and Materials Engineering Department,
Faculty of Engineering, Universiti Kebangsaan Malaysia
43600 Bangi - Selangor D.E., Malaysia
Email: elrdiam@yahoo.com
(Received on 9 Sep 2003, revised on 14 Dec 2003)

Abstract

Correlations of transient heat transfer and pressure drop have been developed for air flowing through the porous media, which packed a double-pass solar air heater. Various porous media are arranged in different porosities to increase heat transfer, area density and the total heat transfer rate. Transient heat transfer experiments indicate that both the heat transfer coefficient and the friction factor are strong functions of porosity. The heat transfer coefficient and the friction factor are also strong functions of the geometrical parameters of the porous media. A test collector was developed and tested indoors by varying the design features and operating conditions using a halogen-lamp simulator as a radiation source. This type of collector can be used for drying and heat applications such as solar industrial processes, space heating and solar drying of agricultural products.

Nomenclature

A	area of the plate (m^2)
B	width of the plate (m)
C	specific heat (KJ/ Kg ^oC)
G	rate of air flow (Kg/hr)
Gr	Grashof number
h	heat transfer coefficient ($W/m^2\,^oC$)
I	solar radiation (W/m^2)
K	conductivity (W/m^oC)
L	length of the plate (m)
m	mass (Kg/m^2)
T	time (sec)
Pr	Prandlt number
Re	Reynolds number
T	temperature
U_R	real loss factor
x	coordinate
α_g	glass absorptivity
δ	thickness (m)
τ	glass transmittance
σ	Stephen's constant ($W/m^2.sec$)
α_p	plate absorptivity
ε	emissivity
η	efficiency
ϕ	porosity
μ	kinematics viscosity of air (Kg/m.sec)
1 and 2	subscripts referring to first and second stream

a	ambient
c	convective
f	fluid
g	glass
p	plate
r	radiative

Introduction

A flat plate air heater experiences a demanding operating environment, which introduces a number of factors to be considered in design of the collector and material selection. Other important factors include solar radiation, temperature and mechanical loading. Most of these collectors used an absorber plate painted dull back to absorb solar radiation and to convert it to heat. Larger channel depth between the absorber and the bottom plate is preferred, because it decreases the heat transfer and pressure drop compared to the lower channel depth. The efficiency of the solar air heater is dependent not only on volumetric airflow rate, but also on air velocity [1].

The main drawback of the flat plate air heater is that the heat transfer coefficient between the absorber and the air stream is low, which results in a lower thermal efficiency of the heater. Hence, different modifications are suggested and applied in order to improve the heat transfer coefficient between the absorber and the air. The modifications included using an absorber with fins attached [2], solid matrix [3], corrugated absorber [4] and hollow spheres [5]. In those works it was emphasized that there was only a pressure drop increase without a proportionate increase in the heat transfer coefficient when the extended surface protruded beyond the sub-layer. Matrawy [6] studied an air heater with a box-type absorber and found that a smaller depth of the channel leads to a higher efficiency, but also to a high-pressure drop through the collector.

Mohamad [7] referred to the conventional double-pass collector as counter-current solar collector, showed that the thermal efficiency can improve by 18% compared to the conventional solar air heater. The study also suggested an extra fan power of 2 to 3 Watts. The losses from the collector include upward loss through the cover plate, back loss through the back of the collector, and the edge loss through the edges of the collector. But the major heat losses from the collector are from the glass cover because the sides, edges and the back of the collector can be insulated adequately, while the front face must be exposed to solar radiation and exposed to the ambient temperature. The temperature of the absorber plate and the glass cover increase in the flow direction, accordingly the thermal loss increases [8]. This paper reports the results obtained from the test of an experimental double-pass solar collector with and without porous media in the lower channel.

Mathematical Model

The heat distribution through the air heater is shown in Fig. 1.

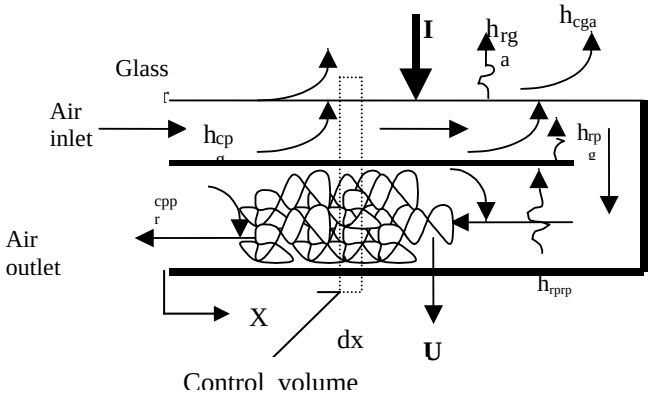

Fig. 1 Schematic of the double-pass solar collector with porous media

Heat balance through the glass cover:

$$m_g C_g \frac{\partial T_g}{\partial t} = \alpha_g I + h_{rpg}(T_p - T_g) + h_{cf,1g}(T_{f,1} - T_g) - h_{(r+c)ga}(T_g - T_a) \quad (1)$$

For air flowing between the glass cover and the plate,

$$m_{f,1} C_{f,1} \frac{\partial T_{f,1}}{\partial t} = -\frac{G_1 C_{f,1}}{B} . \frac{\partial T_{f,1}}{\partial x} + h_{cpf,1}(T_p - T_{f,1}) - h_{cf,1g}(T_{f,1} - T_g) \quad (2)$$

Heat Balance through the absorber plate:

$$m_p C \frac{\partial T_p}{\partial t} = \alpha_p I - K_p \delta_p \frac{\partial^2 T_p}{\partial x^2} - h_{rpg}(T_p - T_g) - h_{cpf,2}(T_p - T_{f,2}) - h_{rppr}(T_P - T_{pr}) - h_{cpf,1}(T_p - T_{f,1}) \quad (3)$$

$$m_{f,2} C_{f,2} \frac{\partial T_{f,2}}{\partial t} = -\frac{G_2 C_{f,2}}{B} . \frac{\partial T_{f,2}}{\partial x} + h_{cpf,2}(T_p - T_{f,2}) + h_{rppr}(T_p - T_{pr}) \quad (4)$$

Heat balance at the bottom:

$$m_b C_b \frac{\partial T_b}{\partial t} = -K_b \delta_b \frac{\partial^2 T_b}{\partial x^2} + h_{rpb}(T_P - T_b) - h_{cbpr}(T_B - T_{pr}) - U_R(T_b - T_a) \quad (5)$$

The boundary conditions are obtained from the conditions that there is no heat loss from the side of the metallic plates. One of the boundary conditions states that at entry point, the air temperature equals the ambient temperature such as:

x = 0, $T_f = T_a$, x =L, $T_f = T_o$).

Numerical calculations were performed for the following values of physical parameters:

B = 1.2 m, L = 2.2m, m_g = 5.5Kg/m^2, m_p = 6.5Kg/m^2, C_a = 1.012 KJ /Kg ^oC, C_g = 0.84 KJ /Kg ^oC, C_p = 0.5 KJ /Kg ^oC, K_p = 47.6N/m^oC, α_g =0.06, α_p = 0.95, δ = 0.004m, and τ_g =0.90

The determination of the average heat transfer coefficient, h , between the porous media and air is as follows:

$$h = mc_p \frac{(\bar{T}_o - \bar{T}_i)}{A(\bar{T}_m - \bar{T}_a)}$$

We now discuss the characteristics of the friction factor for the duct fluid that runs in the collector. An important fundamental relationship is the Fanning equation, given here in a modified form as

$$\Delta P = \frac{4 f W^2 L}{2 g_c A_x^2 \rho D} \quad (6)$$

where ΔP is the frictional loss or pressure drop, W the mass flow rate, L the length of the duct, A_x is cross-sectional area, g_c a constant (1.0Kg.m/Ns^2 or 32.17ft/sec^2), ρ the fluid density, D the equivalent (hydraulic) diameter of the duct and *f* a friction factor. In the case of noncircular cross sections, D is given by

$$De = \frac{4A_x}{p}$$

where P is the perimeter of the duct. The friction factor *f* is as empirical function of the relative roughness of the duct, and the Reynolds number is given by:

$$\mathrm{Re} = \frac{4W}{\mu\pi D}$$

for a smooth duct, when the flow is laminar (Re<2100) the friction factor is given by:

$$f = \frac{16}{\mathrm{Re}}$$

When it is turbulent, for Reynolds number up to about 10^6, friction factor is given by

$$f = 0.00140 + \frac{0.125}{\mathrm{Re}^{0.32}} \tag{7}$$

For rectangular ducts, the pressure drop is given as

$$\Delta p = \frac{fW^2LP\nu}{2g_cA_x^2} = \frac{fW^2LP}{2g_c\rho A_x^3}$$

In many systems pressure drop is most often expressed as the equivalent fluid head loss Δh in terms of meters or feet of water, a convenient fluid for measurement of the pressure drop. In terms of "lost head" of measuring fluid such as water, the equation becomes,

$$\Delta h = \frac{fW^2LP\nu}{2gA_x^3\rho_m} = \frac{fW^2LP}{2g\rho_m\rho A_x^3} \tag{8}$$

Velocity in the ductwork is given by,

$$u = \frac{W}{\rho A_x}$$

Pressure drop or lost head is directly proportional to the length of the duct, proportional to the square of the flow rate, and proportional to the fifth power of the duct size, where the minimum dimensions are most likely to be found. The transmissivity and absorptivity of the glass cover are set to 0.92 and 0.06, respectively. The emissivity of the glass cover and absorber plate is set to 0.92.

The radiative heat transfer coefficient (h_r) is calculated as:

$$h_r = \frac{St(T_1^2 + T_2^2)(T_1 + T_2)}{(\frac{1}{\varepsilon_1} + \frac{1}{\varepsilon_2} - 1)} \tag{9}$$

where *St* is the Stefan-Boltzman constant and subscripts 1 and 2 refer to radiation exchange surfaces [9]. Furthermore, considering that the performance can be expressed by another equation, as

$$\eta = \frac{G.G_p^{'}(T_o - T_i)}{I}$$

This equation can be represented on a single diagram having the same quantities as the abscissa and the ordinates [10].

Experimental Set Up

A schematic diagram of the test rig is shown in Figs. 2 and 3. It essentially consists of a packed bed duct having a length 2.4m with a depth of 0.035 in the first channel and 0.075m at the second channel. In the bed duct the porous media is packed between the absorber plate and the bottom of the collector "second channel". The single glass cover "3 mm thick ordinary glass" was fixed above the absorber plate leaving a space of 3.5cm. The bottom and sides of the test duct have been insulated with 5cm thick fiberglass to minimize heat losses. Copper-constant thermocouples were embedded in the collector sheet at different sections – the absorber plate, the inlet-outlet, the porous media "second channel" and at the glass cover. A micro-manometer was used to measure the pressure drop at the bottom of the flow duct.

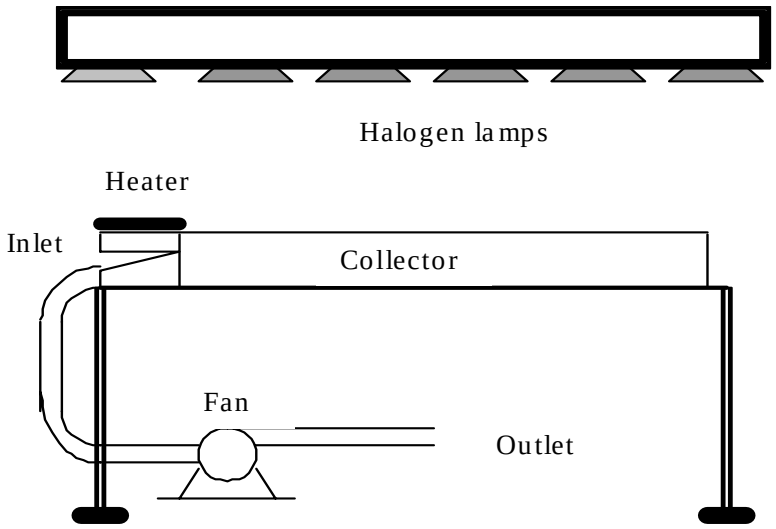

Fig. 2 A schematic diagram of the test rig

Fig 3 A schematic diagram of the test rig.

Beckman [11] recommended standard design dimensions for solar air heating systems. The length of the duct has been recommended to range from 1.25m to 2.5m , the spacing between the absorber plate and the glass cover should range from 1cm to 4 cm. This air heater collector is 2.4m in length and the spacing between the glass and the absorber is 3.5cm. A pyranometer should be fixed at an inclination equal to that the duct to measure the correct intensity of solar radiation falling on the inclined test duct. the solar simulator and the collector undergoing testing. The simulator used 45 halogen lamps, each with a rated power of 300 W. The maximum average radiation was 625 W/m^2, 2.88 m^2 (120x240cm) solar collector in area, 2.64cm^2 (120x220cm) absorber area, and maximum temperature of the absorber exceeded 98 ^oC. For the case of a single glass, 2.88m^2 (120x240cm) in area with a maximum temperature of 45^oC, the maximum outlet temperature exceeded 64^oC and the temperature rises exceeded 23^oC.

The data was collected each half-hour, data include radiation, inlet, outlet , glass cover, absorber plate, porous media and ambient temperatures. The mass flow rate, m, is varied from 0.030Kg/sec to 0.090Kg/sec through the porous media to drying chamber. The collector back was insulated by 5cm of fiber glass, 3mm glass cover (transmissivity 0.85) and black-painted mild steel absorber plate of 0.8mm thickness (absorptivity of 0.9).

Error Analysis

The error analyses during the experiment are as follows:

Mass flow rate about 3.2%, temperature rise about 2.8%, area of the collector according to the measurements is about 1.8%, porosity is about 1.2%, and the pressure drop through the collector (which was measured by manometer error) about 0.5%. The experimental values of thermal efficiency differed from theoretical ones by 6 to 15% as shown in Figs. 4 and 5.

Results and Discussion

In Fig. 4 is shown the mathematical and experimental expressions for the solar radiation effects on the thermal efficiency on the double pass solar collector with the porous media. These effects depend on the surface area of the absorber-plate, which heated the flowing mass. With higher porosity, the increased mass flow rate through this area increased the heat transfer coefficient.

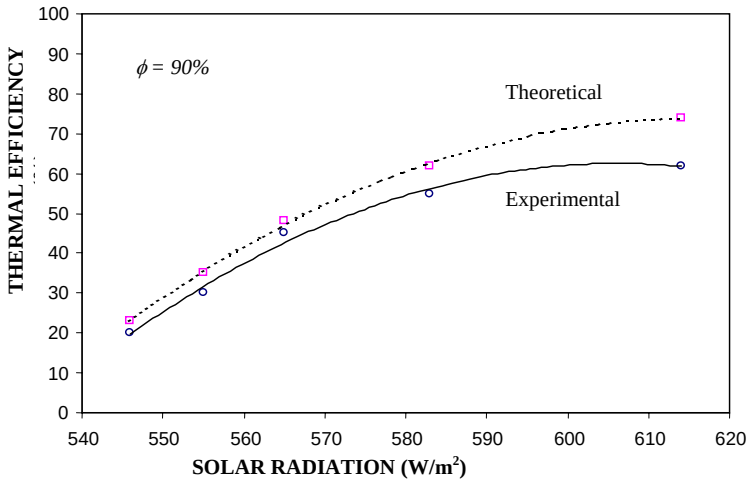

Fig. 4 Effect of the solar radiation on the thermal efficiency on the double-pass solar collector with porous media. (ϕ =90%, T_a= 33.5^{o}C)

In Fig. 5 the effect of mass flow rate on the thermal efficiency is shown compared with the theoretical efficiency. In Fig. 6 is shown the comparison between the theoretical and experimental efficiencies of double-pass solar collector with porous media of different porosities, using of porosity in the second channel increases the heat transfer area and temperature rise, so the efficiency increases as temperature rise increases. In Fig. 7 is shown the effect of mass flow rate on the thermal efficiency of double-pass solar collector with different porosities of porous media. In Fig. 8 is shown the relationship between the temperature rise and the thermal efficiency of double-pass solar collector with porous media.

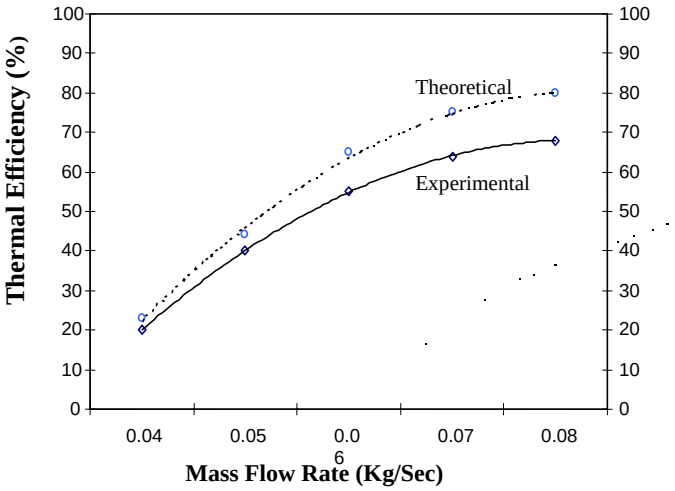

Fig. 5 The effect of the solar radiation on the thermal efficiency on the double pass solar collector with porous media *(ϕ = 80%, T_a= 33.5^{o}C).*

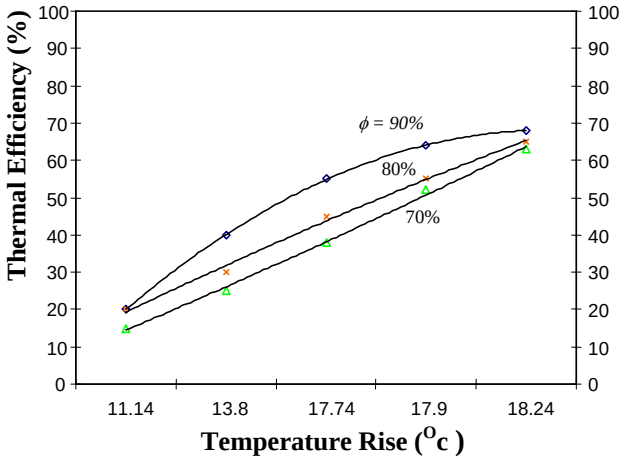

Fig. 6 Effect of temperature rise on the thermal efficiencies of double-pass solar collector with porous media (T_a =33.5^{o}C)

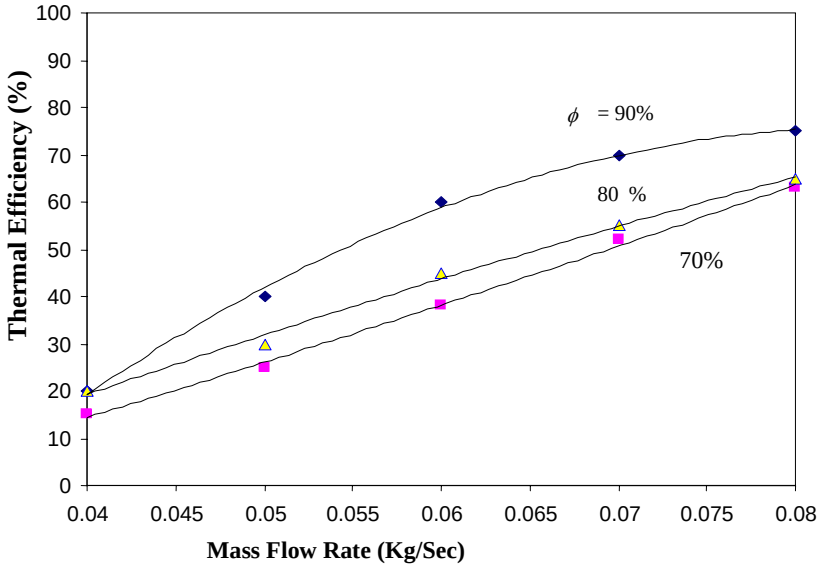

Fig. 7 Effect of mass flow rate on the thermal efficiencies of the double-pass solar collector with porous media (T_a =33.5^{o}C).

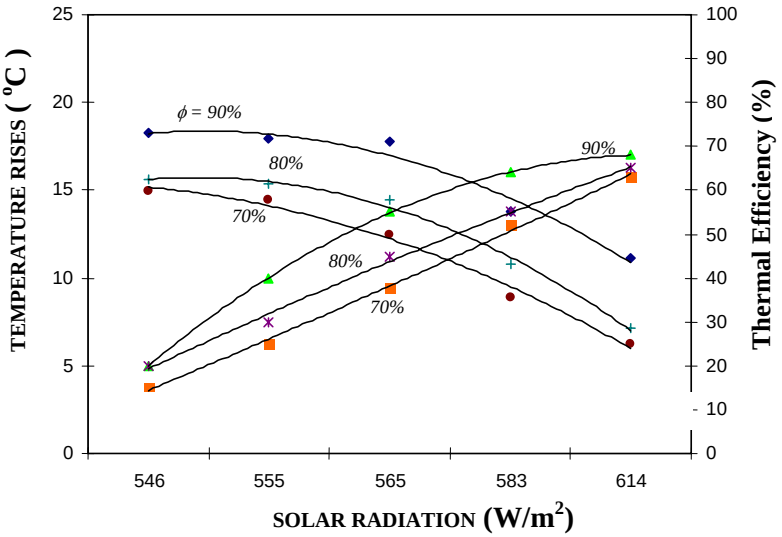

Fig. 8 Effect of solar radiation on temperature rise and thermal efficiencies

Fig. 9 illustrates the effect of the Reynolds number on the pressure drop through the collector, the porous media increases due to the porosity, so pressure drop increases depends on the heat transfer area and temperature rise. Since the porous media was used in the lower channel to increase the heat transfer coefficient, the J-factor depends on the Stanton number, which is directly proportional to the heat transfer coefficient, but the friction factor depends on the losses and velocity of the airflow rate. The pressure drop through the collector depends on the losses such as at the upward edges, the sides and the back.

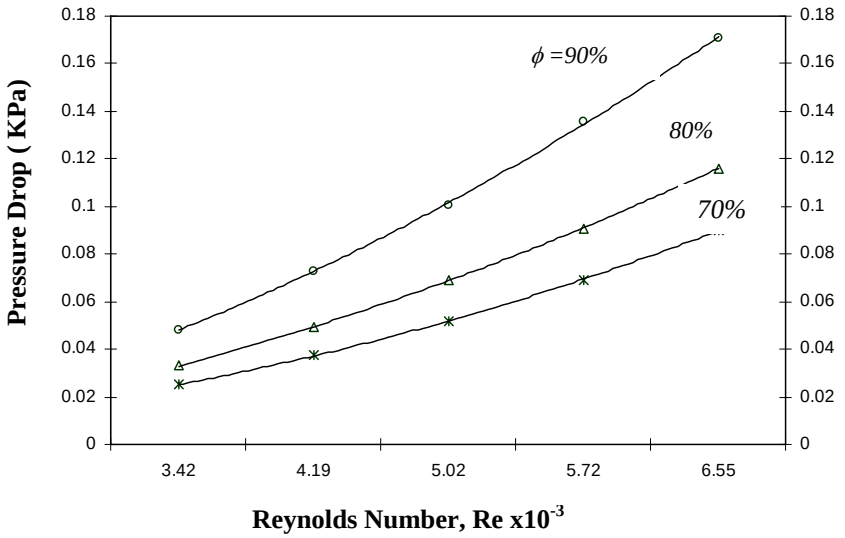

Fig. 9 The effect of Reynolds number on the pressure drop for various porosities of the double pass solar collector with porous media.

Conclusions

In the double-pass solar collector, the mass flow rate has more effect on the temperature rise. The solar radiation has more effect on temperature rises at low porosity. In addition, the Reynolds number has more effect than the Nusselt number at low porosity. Heat transfer coefficient increases by using more porous media in the lower channel of the double-pass solar collector.

Higher porosities in the porous media improved the thermal efficiency. Experimental analysis of the data suggests that due to higher mass flow rate, the thermal efficiency decreases. Pressure drop study indicated that lower pressure losses are encountered with low porosity than with high porosity of the saturated porous media.

Two improved correlations have been developed that may be used to determine the thermal performance of the solar collector with and without porous media. It is shown that the use of experimental data and theoretical simulation greatly simplifies the evaluation of thermal performance of the double pass solar collector with and without porous media.

In order to validate the results, the results of the simulation were compared with the experimental performance of the double pass solar collector with and without porous media, and a favourable agreement was observed.

References

[1] H. P. Garg, "Treatise on solar energy," Fundamental of Solar Energy, Vol. 1, New York, 1982
[2] H. P. Garg, B. Sharma V.K. Bandyopadhyah and A.K Bhargava., "Experimental study and theoretical modeling of solar air heaters for agricultural use, " Solar World Forum "Edited by David O. Hall and June Morton", UK, 1982.
[3] S. P.Sharma, J.S. Saini and H.K. Varma, "Thermal performance of packed-bed solar air heaters," Solar energy, Vol. 47**,** pp 59-67, 1991
[4] C. Choudhury, S.L. Andersen and J. Rekstad, "A solar air heater for low temperature applications," Solar energy, Vol. 40, pp 335-343, 1988.
[5] R. K. Swartman, and O. Ogunade, "An investigation on packed-bed collectors," Solar energy", Vol. 10, pp 106 – 110, 1996.
[6] K. K. Matrawy, "Theoretical Analysis for an air Heater with a Box- type absorber," Solar energy, Vol. 63, pp 191-198, 1998.
[7] A. A. Mohamad, "Counter-current solar air heater, Proc. Karadeniz Technical University, Trabzon, pp. 129 – 134, Turkey, 1996.
[8] A. A. Mohamad, "High efficiency solar air heater, Solar energy, Vol. 60, pp. 71-76, 1997.
[9] A. Willier, "Performance of black painted solar air heaters of conventional design," Solar energy, Vol. 8, pp 31-37, 1964.
[10] T. A. Ready and C. L.Gupta, "Generating application design data for solar air heating systems," Solar energy, Vol. 25, pp 527-530, 1980
[11] W. Beckman, S. A. Klein and J. A. Duffie, "Solar heating design by the f-chart method," WILEY, New York, 1997.